

# Ionic Modulation of Atrial Fibrillation Dynamics in a Human 3D Atrial Model

C Sánchez<sup>1,2,3</sup>, MW Krueger<sup>4</sup>, G Seemann<sup>4</sup>, O Dössel<sup>4</sup>, E Pueyo<sup>2,1</sup>, B Rodríguez<sup>3</sup>

<sup>1</sup> Communications Technology Group, I3A, University of Zaragoza, Zaragoza, Spain

<sup>2</sup> Biomedical Research Networking Center in Bioengineering, Biomaterials and Nanomedicine (CIBER-BBN), Spain

<sup>3</sup> Computational Biology Group, Oxford University Department of Computer Science, Oxford, UK

<sup>4</sup> Institute of Biomedical Engineering, Karlsruhe Institute of Technology (KIT), Karlsruhe, Germany

## Abstract

*Atrial fibrillation (AF) is the most common cardiac arrhythmia, and is mainly sustained by reentrant circuits and rapid ectopic activity. In the present study, we performed computer simulations using a 3D human atrial model including fibre orientation, electrophysiological heterogeneities and tissue anisotropy. Membrane kinetics were described as in the human atrial action potential model by Maleckar et al., including AF-induced ionic remodeling. The impact of ionic changes on reentrant activity was investigated by characterizing arrhythmia stability, rotor dynamics and dominant frequency (DF). Our simulations show that reentrant circuits tend to organize around the pulmonary veins and the right atrial appendage. Simulated  $I_{K1}$  and  $I_{Na}$  blocks lead to slower DF in the whole atria, expanded wave meandering and reduction of secondary wavelets.  $I_{NaK}$  block slightly reduces DF and does not notably change the propagation pattern. Regularity and coupling indices of electrograms are usually higher in the right atrium than in the left atrium, entailing a higher likelihood of arrhythmia generation in the latter, as occurs in AF patients.*

## 1. Introduction

Atrial fibrillation (AF) is the most commonly diagnosed arrhythmia and its mechanisms of generation and maintenance have been widely studied. It is well established that AF normally arises by rapid ectopic activity around the pulmonary veins generating stable reentrant circuits combined with short duration wavelets that propagate through the whole atria creating a chaotic activation that may then affect the ventricular pacing. Furthermore, persistent AF leads to physical changes, such as atrial dilation, and electrophysiological remodeling of ion channels (AFER) favoring fibrillatory behavior by long circuit pathways, slow conduction and short refractory periods.

The objective of this study is to analyze the effects of ionic changes on simulated arrhythmias using a realistic human atrial 3D model [1]. Electrophysiology of cells composing the 3D model is simulated using the Maleckar et al. action potential (AP) model [2]. Computational simulations are validated using experimental data from the literature.

## 2. Methods

### 2.1. Model specifications

The human atrial AP model developed by Maleckar et al. [2] is embedded in a realistic 3D atrial geometry [1] to investigate the impact of changes in certain ionic properties in modulating arrhythmic markers in AFER conditions. AFER is simulated by altering ion channel conductances as described in previous studies [3]: 70%  $I_{CaL}$  reduction; 50%  $I_{to}$  reduction; 50%  $I_{Kur}$  reduction; and 100%  $I_{K1}$  increment. Effects of the parasympathetic activity are simulated by including 1 nM of acetylcholine concentration ([ACh]) through an ACh-activated potassium current ( $I_{KACh}$ ) [4]. To assess the relevance of the [ACh] level, simulations including 5 nM are also analysed. The 3D model contains the main atrial structures: left atrium (LA), right atrium (RA), sinoatrial node (SAN), cresta terminalis (CT), pectinate muscles (PM), fossa ovalis (FO), Bachmann's bundle (BB), cavotricuspid isthmus (CTI), left atrial appendage (LAPG), right atrial appendage (RAPG), atrioventricular ring (AVR) and interatrial bridges (IAB). Furthermore, the model includes fiber orientation, conduction anisotropy and spatial heterogeneities in both ionic currents and conduction velocity (CV) [1, 5]. Anisotropic ratio (transversal to longitudinal ratio of conductivity) and spatial heterogeneities are summarized in Table 1. LA-RA gradients are simulated by including differences in  $I_{Kr}$  (1.6 times greater in LA than RA) and  $I_{KACh}$  (2 times greater in LA than RA) according to previous studies [6].

Table 1. Tissue anisotropy and heterogeneities.

	Anisotropic ratio	CV (cm/s)	$I_{to}^*$	$I_{CaL}^*$	$I_{Kr}^*$	$I_{KACH}^*$
LA	1:2	59	1	1	$\sqrt{1.6}$	$\sqrt{2}$
RA	1:2	59	1	1	$1/\sqrt{1.6}$	$1/\sqrt{2}$
SAN	1:1	31	1	1	1	1
CT	1:10	116	1.35	1.6	0.9	1
PM	1:2	98	1.05	0.95	0.9	1
FO, RAPG, IAB	1:2	59	1	1	1	1
BB	1:2	98	1	1	1	1
CTI	1:1	44	1	1	1	1
LAPG	1:2	59	0.65	1.05	2.75	1
AVR	1:2	59	1.05	0.65	3	1

\*Multiplicative factors with respect to default values in the model

## 2.2. Stimulation protocol

Atrial cells within the 3D model are stimulated using 2-ms duration and twice diastolic threshold current pulses. A preliminary conditioning of the 3D model is performed by applying a train of 40 periodic stimuli at the SAN cells at a cycle length (CL) of 500 ms. Then, 6 extra-stimuli are applied around the right pulmonary veins (RPV) to generate reentries and fibrillatory behavior. Simulations are run using the finite element method described in [7].

## 2.3. Simulation analysis

Single blocks of the most relevant ionic currents modulating single cell and tissue properties [8] are simulated:  $I_{K1}$  (-30%),  $I_{Na}$  (-15%) and  $I_{NaK}$  (-30%). Notice stronger  $I_{Na}$  blocks would result in less excitable tissue that could lead to propagation failure.

Characterization of the arrhythmia simulations is performed by mapping LA and RA with 49 virtual electrodes, separated approximately 1 cm from their closest neighbour and 0.1 cm from the atrial surface. The corresponding pseudo-electrograms (pEGM) for each simulation are calculated at the electrodes as in a previous study [9]. In order to evaluate regularity and organization, some properties are measured on the pEGM: the dominant frequency (DF), the regularity index (RI) and the coupling between adjacent pEGM (CP), obtained as in [10].

## 3. Results

### 3.1. Parasympathetic effects

As shown in Figure 1, the level of [ACh] leads to different propagation patterns through the atria. When [ACh] is set to 1 nM, the reentrant behaviour is sustained by two main rotors located near the RPV and the RAPG, whereas when [ACh] is 5 nM, there is one main rotor at the RAPG

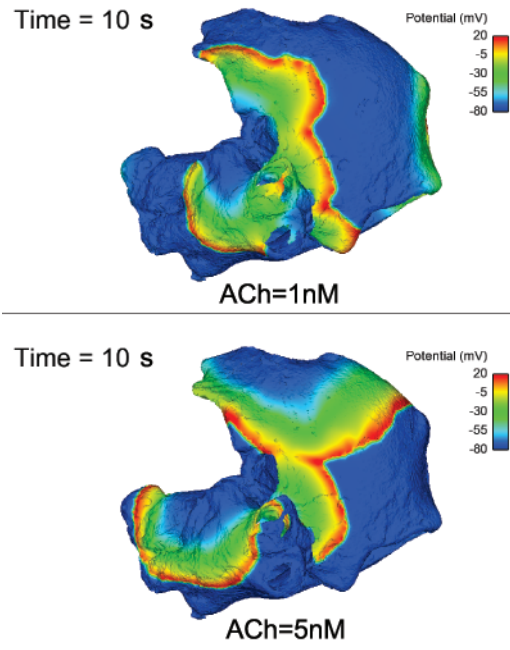


Figure 1. Dorsal view of the atria. Transmembrane potential map after 10 seconds of simulation for default conditions (AFER) when [ACh]=1 nM (upper panel) and 5 nM (lower panel).

and a few secondary rotors lasting a few seconds (around the left pulmonary veins (LPV)) or being blocked by the main rotor (superior vena cava (SVC), mitral valve (MV)). DF distribution throughout the tissue is almost uniform due to the highly stable rotors when both [ACh] levels are simulated, but in average its value is slightly reduced for 5 nM (DF around 5.86 Hz) compared to 1 nM (DF around 6.15 Hz). Regarding RI and CP, they are generally much lower when [ACh] is 5 nM due to the effects of temporary rotors on closely located pEGM morphology.

### 3.2. Ionic modulation

The effects of alterations in the ionic mechanisms unraveled in previous studies on AF dynamics are investigated so that their usefulness as potential targets for anti-AF drugs can be evaluated. As expected from previous studies on cell and tissue properties [8],  $I_{K1}$ ,  $I_{Na}$  and  $I_{NaK}$  modulate fibrillatory properties and rotor dynamics. It is important to remark that, once the re-entrant wavefronts are generated following the stimulation protocol, the fibrillatory behavior remains self-sustained for the duration of the simulation. Figure 2 shows similar transmembrane potential map patterns following 10 seconds of simulation for default conditions (AFER), 30%  $I_{K1}$  block, 15%  $I_{Na}$  block and 30%  $I_{NaK}$  block. The centers of the main rotors are usually located near the RPV and the RAPG, and secondary rotors usually appear close to the SVC and the MV.

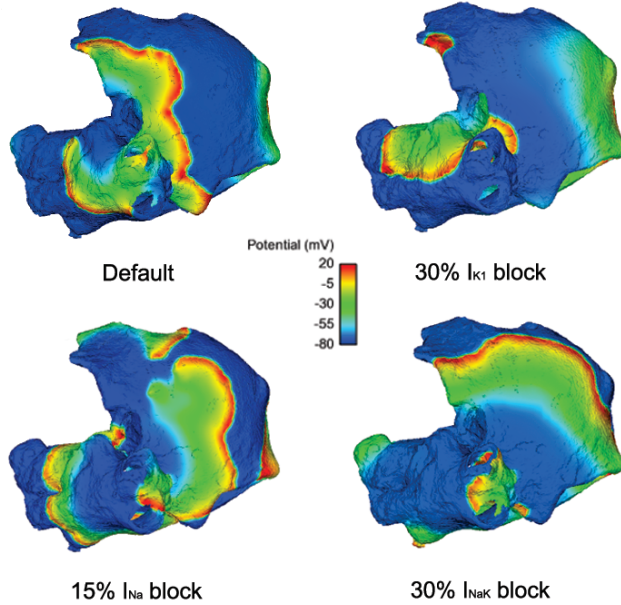


Figure 2. Dorsal view of the atria. Transmembrane potential map after 10 seconds of simulation for default conditions (AFER), 30%  $I_{K1}$  block, 15%  $I_{Na}$  block and 30%  $I_{NaK}$  block, respectively.

Regarding DF results, its distribution is very homogeneous in all the simulations because the main rotors predominate over possible secondary rotors entailing certain periodicity of cell activation in all the atrial tissue. Block of  $I_{Na}$  leads to significantly smaller DF values (5.27 Hz in average), whereas  $I_{K1}$  and  $I_{NaK}$  blocks reduce DF slightly (5.66 Hz and 5.76 Hz, respectively, in average).

The organization of the arrhythmia is analysed by obtaining RI and CP indices on the pEGM. Figure 3 shows maps of the 49 RI obtained from the pEGM and their inter-

polation for all the cells in the model. Block of  $I_{K1}$  leads to a slight increase in RI around the RPV, but reduces organization in the LA. In contrast, inhibition of  $I_{Na}$  significantly increases organization in the LA, but reduces RI in the RA. Block of  $I_{NaK}$  notably reduces RI in both atria.

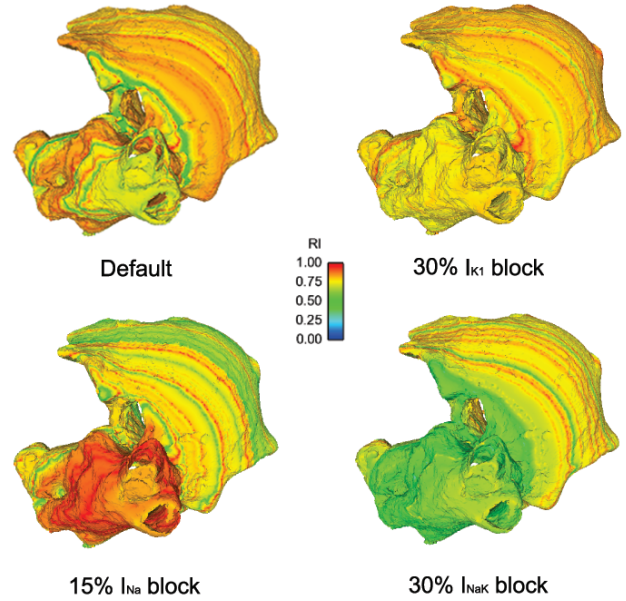


Figure 3. Dorsal view of the atria. Interpolated RI map for default conditions (AFER), 30%  $I_{K1}$  block, 15%  $I_{Na}$  block and 30%  $I_{NaK}$  block, respectively.

In good agreement with RI results, Figure 4 shows that CP indices are slightly reduced in both the LA and the RA when  $I_{K1}$  is blocked, block of  $I_{Na}$  leads to high coupling in the LA but is significantly reduced in the whole RA, and inhibition of  $I_{NaK}$  significantly reduces coupling in the LA and slightly in the RA.

## 4. Discussion and conclusions

This study confirms the importance of the parasympathetic system, through the inclusion of [ACh], on the modulation of AF dynamics. High levels of [ACh] significantly shorten both cellular AP duration and tissue refractory periods thus allowing several wavelets to propagate simultaneously as occurs in AF [4]. Our simulations show that high [ACh] levels promote disorganization of arrhythmia despite not entailing very significant changes in DF.

Furthermore, in this study we confirm the relevance of certain ionic currents in determining arrhythmic markers (DF, RI and CP). These markers can also be used in clinical practice with real electrograms in order to guide anti-arrhythmic therapies, such as ablation procedures. The

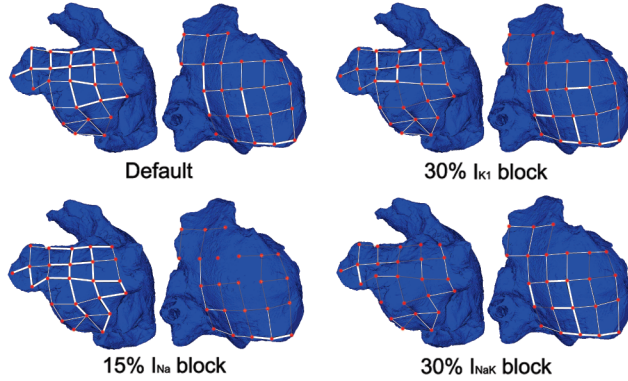


Figure 4. Coupling between pEGM in adjacent electrodes for the LA (left) and the RA (right). Thick white lines represent  $CP \geq 0.9$ , thin solid lines represent  $0.75 \leq CP < 0.9$  and soft gray lines represent  $0.6 \leq CP < 0.75$ .  $CP < 0.6$  is represented by line absence.

main advantage of this technique is the capability of fully characterize the whole atria with only 49 electrodes.

Regarding the ionic current effects studied, changes in  $I_{Na}$  and, to a lesser extent,  $I_{K1}$  and  $I_{NaK}$  induce important effects on arrhythmogenicity of atrial tissue. Their inhibition leads to antiarrhythmic decrease of DF, more prominent when the inhibited ionic current is  $I_{Na}$  than when  $I_{K1}$  or  $I_{NaK}$  are blocked. Organization and regularity of fibrillatory waves are increased in the LA if a block of  $I_{Na}$  is simulated, whereas  $I_{K1}$  or  $I_{NaK}$  blocks lead to more disorganized electrical propagation in the LA. In contrast, blocks of  $I_{K1}$  or  $I_{NaK}$  maintain organization of the waves in the RA, whereas  $I_{Na}$  inhibition reduces RI and CP in this chamber.

Previous studies have remarked that smaller  $I_{K1}$  in human atria may lead to deceleration and decreased stability of rotors, as occurs in our study, but entails depolarized resting potential associated with increased susceptibility to arrhythmias [11].

$I_{Na}$  block effectively slows down CV, increases the wavelength of reentrant circuits and reduces DF [3], in agreement with the results of the present study. However, the possible side effects on ventricular electrophysiology of sodium channel blockers highlight the necessity of finding atrial selective therapies.

Regarding  $I_{NaK}$ , it is shown that the effects of alterations in the  $Na^+/K^+$  pump in atrial tissue induce slight effects on fibrillatory dynamics and organization, despite its key role on cellular AP duration and rate adaptation [8].

In this study, the role of ionic currents in modulating atrial fibrillation dynamics in a realistic 3D atrial model is investigated. Simulations confirm the potential interest of developing atrial selective anti-AF drugs aiming at inhibiting either  $I_{K1}$  or  $I_{Na}$  or  $I_{NaK}$ .

## Acknowledgements

This study was financially supported by the European Commission preDiCT Grant DG-INFSo-224381 (to B.R.), grant TEC-2010-19140 from Ministerio de Economía y Competitividad (MINECO), Spain, and fellowship BES-2008-002522 from MINECO, Spain (to C.S.). E.P. acknowledges the financial support of Ramón y Cajal program from MINECO. The research leading to these results has received funding from the European Community Seventh Framework Programme (FP7/2007-2013) under grant agreement no 224495 (euHeart project).

## References

- [1] Seemann G, Höpper C, Sachse FB, Dössel O, Holden AV, Zhang H: Heterogeneous three-dimensional anatomical and electrophysiological model of human atria. *Phil Trans R Soc A* 2006;364:1465–1481.
- [2] Maleckar MM, Greenstein JL, Giles WR, Trayanova NA:  $K^+$  current changes account for the rate dependence of the action potential in the human atrial myocyte. *Am J Physiol Heart Circ Physiol* 2009;297:H1398–H1410.
- [3] Pandit SV, Berenfeld O, Anumonwo JMB, Zaritski RM, Kneller J, Nattel S, Jalife J: Ionic determinants of functional reentry in a 2-D model of human atrial cells during simulated chronic atrial fibrillation. *Biophys J* 2005;88:3806–3821.
- [4] Kneller J, Zou R, Vigmond EJ, Wang Z, Leon LJ, Nattel S: Cholinergic atrial fibrillation in a computer model of a two-dimensional sheet of canine atrial cells with realistic ionic properties. *Circ Res* 2002;90:e73–e87.
- [5] Krueger MW, Schmidt V, Tobón C, Weber FM, Lorenz C, Keller DUJ, Barschdorf H, Burdumy M, Neher P, Plank G, Rhode K, Seemann G, Sánchez-Quintana D, Saiz J, Razavi R, Dössel O: Modeling atrial fiber orientation in patient-specific geometries: a semi-automatic rule-based approach. *FIMH 2011, LNCS 6666*:223–232.
- [6] Atenza F, Almendral J, Moreno J, Vaidyanathan R, Talkachou A, Kalifa J, Arenal A, Villacastín JP, Torrecilla EG, Sánchez A, Ploutz-Snyder R, Jalife J, Berenfeld O: Activation of inward rectifier potassium channels accelerates atrial fibrillation in humans: evidence for a reentrant mechanism. *Circulation* 2006;114:2434–2442.
- [7] EA, Ferrero JM, Doblaré M, Rodríguez JF: Adaptive macro finite elements for the numerical solution of monodomain equations in cardiac electrophysiology. *Ann Bio Eng* 2010;38(7):2331–2345.
- [8] Sánchez C, Corrias A, Bueno-Orovio A, Davies M, Swinton J, Jacobson I, Pueyo E, Rodríguez B: The  $Na^+/K^+$  pump is an important modulator of refractoriness and dynamics in human atrial tissue. *Am J Physiol Heart Circ Physiol* 2012;302:H1146–H1159.
- [9] Baher A, Qu Z, Hayatdavoudi A, Lamp ST, Yang MJ, Xie F, Turner S, Garfinkel A, Weiss JN: Short-term cardiac memory and mother rotor fibrillation. *Am J Physiol Heart Circ Physiol* 2007;292:H180–H189.
- [10] Faes L, Ravelli F: A morphology based approach to the evaluation of atrial fibrillation organization. *IEEE Eng Med Biol Mag* 2007;26(4):54–59.
- [11] Ehrlich JR: Inward rectifier potassium currents as a target for atrial fibrillation therapy. *J Cardiovasc Pharmacol* 2008;52:129–135.

Address for correspondence:

Carlos Sánchez  
DIEC / I3A / University of Zaragoza / Spain  
cstapia@unizar.es